Stability, Dynamics, and Origins of the υ Andromedae Planetary System

Verene J. Lystad

Department of Physics and Astronomy, Northwestern University, Evanston, IL 60208

May 13, 2005

ABSTRACT

Since the announcement of the triple planet system orbiting Upsilon Andromedae (υ And) by Butler et al. in 1999, the best-fit orbital parameters of the system have varied significantly with additional observations over the years. Using the most recent radial velocity data we have performed thousands of numerical integrations to survey the allowed parameter space for stable orbital configurations. For all allowed solutions, we find that the eccentricity of the outer planet (planet d) oscillates between about 0.25 and 0.35, while the middle planet (planet c) periodically returns to a very nearly circular orbit every 6700 years. Several mechanisms have been proposed to explain the unexpectedly large eccentricities of known extrasolar planets, but as yet there has been little direct observational evidence to support any one theory. The configuration of υ And provides evidence that planet-planet scattering must be responsible for the large eccentricities observed in this system. The planets initially started on circular orbits, as expected from our current understanding of planet formation, but chaotic evolution caused planet d to be perturbed suddenly into a higher eccentricity orbit, subsequently causing planet c's eccentricity to oscillate as it is observed at present. The impulsive perturbation resulted most likely from a close encounter with another planet, now lost from the system.

1. Introduction

In the ten years since the discovery of the first extrasolar planet around 51 Peg (Mayor & Queloz 1995), a total of 155 extrasolar planets have now been identified, in 136 planetary systems (Schneider 2005). In 1999 the planetary system around Upsilon Andromedae (υ And) was the first triple planet system to be found and, as such, has provided a unique and truly invaluable foundation on which to study the formation and dynamics of multiple planet systems. Until 1995 all theories of planetary formation and dynamics were developed with our own Solar System as the sole model. However, particularly after the discovery of multiple planet systems like υ And, our increasing awareness of the many ways in which properties of known extrasolar planets differ from those in the Solar System has catalyzed significant reevaluations of these theories and subsequently revolutionized our understanding of this area of Astrophysics. The study of extrasolar planets addresses significant problems regarding not only the origins of planetary systems, but also the conditions surrounding the hospitality of life on Earth, as well as outside the Solar system, and thus may lend insight into just how common or unique humanity's place in the universe may be.

This thesis is organized as follows: In the remainder of this section we discuss the limitations of the observational data with specific attention to the υ And system. We also discuss how orbital information not yeilded by observation can, however, potentially be recovered through numerical integration. In section 2 [1] we discuss considerations and approaches to our own examination of the υ And system. Section 3 details the results of our numerical integrations. Specifically, we find constraints on the unknown angles of inclination, which are used to determine upper mass limits for the planets, and we discuss evidence for planet-planet scattering in the system. Finally in Section 4 we consider the ramifications of our findings on the evolutionary history of the system.

1.1. Detection Methods and Limitations

The process of detecting planets can be somewhat tricky and unfortunately leads to biases in the characteristics of planets discovered. Telescopic resolution imposes a severe limitation on detection by direct imaging or astrometry, and thus only a few extrasolar planets have been found or confirmed using these methods. Searches for planets have also been carried out by continuously monitoring hundreds of stars in hopes of detecting the transit of a planet, indicated by a brief and minute decrease in the brightness of the star at regular intervals. Given the small probability that a planet's orbit would cause it to cross precisely within our line of sight to the star, this also remains an inefficient method of

---

[1] Sections 2 through 4 are based on the paper: Ford, E.B., Lystad, V., & Rasio, F.A. "Planet-Planet Scattering in Upsilon Andromedae," 2005, *Nature*, 343, 873. My contributions to this work were centered primarily on the numerical integrations of the υ And system. Starting from the initial conditions generated from the radial velocity curve, I ran more than 7000 integrations with each set of 1000 having distinct specifications for initial angles of inclination, as well as the 1500 integrations for systems including hypothetical planets e and f, along with planets c and d, all starting on circular orbits. I then wrote programs to aid in the statistical analyses of these systems and generated plots for interpretation and presentation.

searching for extrasolar planets.

Currently Doppler spectroscopy is the favored detection method in large-scale planet searches, though it is not without its own disadvantages. With Doppler spectroscopy observers measure periodic shifts in a star's spectrum, yielding a radial velocity curve produced by the small gravitational perturbations of an orbiting planet (or planets). Fourier transforms applied to the radial velocity curve isolate the individual orbits in a multiple-planet system. Each radial velocity curve is fitted approximately by a Keplerian sinusoid, which takes the form

$$V = K[\cos(f+\omega) + e\cos\omega]$$

where f is the planet's true anomaly (see Table 1 for a complete discription of orbital elements), ω is the argument of pericenter, e is the orbital eccentricity, and K is the semi-amplitude. For a planet of mass m orbiting a star of mass $M_\star$ with a semimajor axis a, the semi-amplitude of the radial velocity curve is given by

$$K = \frac{m\sin i}{M_\star + m}\sqrt{\frac{G(M_\star + m)}{a(1-e^2)}}.$$

The time of pericenter passage $T_{\rm peri}$ and the period P of the orbit can also be found directly from the radial velocity curve.

Radial velocity curves only give one component of the orbital motions, along the line of sight. Thus, the inclination with respect to the line of sight i (where edge-on corresponds to $i = 90°$) and the longitude of pericenter Ω, which gives the inclination perpendicular to i, cannot be measured directly. From Kepler's third law

$$\frac{a^3}{GM_\star} = \left(\frac{P}{2\pi}\right)^2,$$

the radial velocity curve only provides a lower limit on the planetary mass by fixing the value of $m\sin i$. Numerical integrations of planetary orbits can place upper limits on the true masses by requiring the system to remain stable on timescales comparable to the lifetime of the central star (see §1.2.4). Since systems tend to go unstable more often with increasing planetary masses, there is generally a maximum i, as well as a maximum relative inclination $i_{\rm rel}$. It is worthwhile to note that the relative inclination between any two planets, denoted by subscripts 1 and 2, is equal to

$$i_{\rm rel,12} = \cos i_1 \cos i_2 + \sin i_1 \sin i_2 \cos(\Omega_1 - \Omega_2)$$

(Malhotra 2002). In the case that $\Omega_1 = \Omega_2$, this equation reduces to $i_{\rm rel,12} = i_1 - i_2$.

The semi-amplitude of the radial velocity curve is a direct consequence of the gravitational forces acting between the star and the planet,

$$F = \frac{GM_\star m}{r^2}$$

where G is the gravitational constant, $M_\star$ is the mass of the central star, m is the mass of the planet, and r is the distance separating the star and the planet. Since this force increases with larger m and smaller r, planets with more mass and little separation from the central star are therefore much easier to detect through a star's radial velocity curve. Despite its limitations and biases, Doppler spectroscopy remains the most efficient method for detecting extrasolar planets.

1.2. Background Data and Theory

1.2.1. Overview of Extrasolar Planetary Data

Most known planets are quite massive ($m \sin i$ is usually a few M_J, where $1M_J$ is definied to be the mass of Jupiter) and have small semimajor axes relative to the planets in our Solar System. A major question facing theorists is how to explain the existence of these so-called "hot Jupiters" at such remarkable proximity to the central star. Furthermore, the known extrasolar planets on orbits $\lesssim 0.15$ AU tend to have small orbital eccentricities due to tidal circularization by their central star (Rasio et al. 1996), however the majority of extrasolar planets in fact have quite large eccentricities. Of the 155 planets known to date (Schneider 2005), the 104 planets with semimajor axes greater than 0.15 AU (large enough to avoid the effects of tidal circularization) have an average eccentricity of 0.35. This is in stark contrast to the eccentricities found in our own Solar System; all are below 0.1, with the exception of Mercury and Pluto. The largest eccentricity among the gas giants in the Solar System is Saturn's at $e = 0.054$.

1.2.2. Standard Theory for Planetary Formation

The observed properties of the orbits of extrasolar planets are especially puzzling when considered in the context of the standard core accretion model for giant planet formation in our Solar System (see, e.g., Lin & Ida 1997; Laughlin & Chambers 2001). In this model giant planets form from the same protostellar disk as the central star, by gradually accumulating planetesimals into a $\sim 10M_\oplus$ core (where $1M_\oplus$ is defined to be the mass of the Earth). This phase is followed by a period of gravitational accretion of a gaseous envelope from material in the surrounding protostellar nebula (Pollack et al. 1996), consequently leaving a gap in the disk along the path of the planet's circular orbit. According to this theory, giant planets should only be found at distances greater than about 4AU from the central star, where the temperature in the protostellar nebula is low enough to allow icy materials to condense (Boss 1995). Thus, it was quite unexpected that the vast majority of extrasolar planets have large eccentricities and orbit so close to their central stars, given that they are so massive.

1.2.3. Data on υ And

In 1999 υ And was announced to be the first known multiple-planet system (Butler et al. 1999). The central star, upsilon Andromedae, is an F8 V star with a mass between $1.2 - 1.4M_{\odot}$, and an age of about 2-3 Gyr (Ford, Rasio, & Sills 1999). Since its discovery, this triple planet system has been the focus of many theoretical studies to investigate its stability and dynamics (see e.g. Laughlin & Adams 1999; Lissauer & Rivera 2001; Barnes & Quinn 2001) as well as the possible presence of secular resonance between the outer two planets (planets c and d) (see e.g. Stepinski, Malhotra, & Black 2000; Chiang, Tabachnik, & Tremaine 2001). Partly as a consequence of ongoing interest in this system, the California and Carnegie Planet Search team has now taken over 350 radial velocity measurements, making this system among those with the most tightly constrained orbital parameters.

Table 2 shows the most up-to-date orbital parameters derived from the entire Lick Observatory data set, kindly provided by Debra Fischer (private communication 2004), for all three planets in the system: planets b, c, and d, in order of increasing periods. These values may be compared with those in Table 3 of the previously most up-to-date published orbital parameters, now two years old (Fischer et al. 2003). Note in both tables that the eccentricities of planets c and d are both quite large relative those of the gas giants in our Solar System, as is consistent with eccentricities of most other extrasolar planets.

In the 2003 parameters, and indeed in all previously published sets of orbital parameters, the longitudes of pericenter for planets c and d, ϖ_c and ϖ_d, appeared to be quite close to each other, at times with the 1-σ uncertainties overlapping. On the surface this remarkable proximity seemed least surprising if the two planets were in secular resonance (also called apsidal resonance), meaning specifically that the difference in longitudes of pericenter $|\varpi_c - \varpi_d|$ oscillate with small amplitude. (Following the usual nomenclature, we say the planets are librating as long as $|\varpi_c - \varpi_d|$ is oscillating, regardless of amplitude; if instead $|\varpi_c - \varpi_d|$ passes through all angles from 0 to 360°, we say they are circulating. In the librating configuration, the libration amplitude is the maximum value of $|\varpi_c - \varpi_d|$.) Furthermore, in order for the planets to be locked in secular resonance, their orbits would have to lie in nearly the same plane; thus the proximity of ϖ_c and $varpi_d$ also implies near coplanarity of the orbits. Comparing the values in Table 2 with those in Table 3, the current value of $|\varpi_c - \varpi_d|$ is still relatively small, though notably not as small as previously observed.

In addition to the orbital properties of the υ And system revealed through the radial velocity curve of the central star, the absence of transits implies that $i_b < 83°$ (Henry et al. 2000). Additionally, Hipparcos astrometry data reveals that $i_d > 11.5°$ (Mazeh et al. 1999), thus indicating that the mass of planet d is $\lesssim 5$ times the observed lower limit. These measurements will help to constrain the masses of all the planets in υ And if the system is found by theoretical arguments to be nearly coplanar.

1.2.4. Previous Studies of υ And

According to standard theory of planet formation, since the planets form out of the same disk as the central star, it can be assumed that the ages of the planets must be similar to that of the star. The system must necessarily be stable on these timescales; certainly if it were not, then it would not have survived to be observed at present. For fixed semimajor axes, multiple-planet systems tend to go unstable more quickly as the masses of the planets increase (Gladman 1993). Thus, through numerical integration for the lifetime of the star, it is possible to find upper mass limits, as well as upper limits on relative inclinations between planets. However, as we will show, this does not necessarily indicate that the history of the planetary system must have been entirely uneventful.

Many research groups to study this system previously have given values for these limits. However, as more observations of the system are made and the best-fit parameters are adjusted accordingly, the values for these limits vary. For example in 1999, Laughlin & Adams found that i was unlikely to fall below about 40°, thus restricting the planets' masses to $\lesssim 1.5$ times the measured minimum values. They also found that the system favors relative inclinations between the outer two planets of about $15 - 20°$. By contrast, Lissauer & Rivera (2001) find, that the system is stable for up to 4 times the minimum planetary masses and that it is most stable for nearly coplanar configurations.

Several previous studies of the υ And system report the presence of secular resonance between planets c and d, meaning specifically that the system is librating with small amplitude. For example, Chiang, Tabachnik, & Tremaine (2001) find that almost all stable orbital configurations with initial conditions within the allowed observational errors exhibit secular resonance. Further, they claim that the system is dependent on the presence of secular resonance in order to remain stable for the duration of their integrations. While not all groups to study the υ And system found the stability of the system to be so highly correlated with secular resonance, many believed such a resonant configuration was in fact the best explanation for the apparent small separation between ϖ_c and ϖ_d. Some groups even searched specifically for initial orbital configurations that would produce secular resonances with the smallest possible libration amplitude (see, e.g., Lissauer & Rivera, 2001).

By contrast, Stepinsky, Malhotra & Black (2000) found that there is no secular resonance in the system. Barnes & Quinn (2001) claim that, although planets c and d are in secular resonance for some allowed configurations, the stability of the system does not depend on the presence of this resonance, and therefore that the observed proximity of the longitudes of pericenter for planets c and d is most likely coincidental. It seemed that the debate over the presence of secular resonance in the υ And system would have no simple resolution; the methods behind the claims of every group may have been perfectly sound, but the reliability of any results ultimately depends on the accuracy of the radial velocity measurements.

Additionally, it was also quickly recognized after the discovery of the three planets in the υ And system that the gravitational interaction between the outer two planets causes significant eccentricity evolution on secular timescales ($\sim 10^4$ years). In particular, in some early solutions, the middle planet appeared to have its eccentricity varying periodically with large amplitude, from a maximum near the present value to a minimum near zero (Stepinsky, Malhotra, & Black 2000).

2. Methods

2.1. Stability Criteria

For planetary systems containing two planets, the stability of the system for all time can be determined using analytical criteria (Hill 1878). Specifically, the Hill stability criterion in the limit of small eccentricities indicates that, as long as the separation between the semimajor axes of two planets satisfies

$$|a_1 - a_2| > \frac{2}{\sqrt{3}} R_H,$$

where R_H is the Hill radius of the planets defined to be

$$R_H \equiv \left(\frac{a_1 + a_2}{2}\right) \left(\frac{m_1 + m_2}{3M_\star}\right)^{1/3},$$

where subscripts specify parameters for each planet, then the two planets will remain stable against close encounters. Unfortunately no analytical stability criterion exists for systems containing more than two planets; in fact systems of more than two planets are always chaotic and formally unstable. In general, the stability of N-body systems must be determined through direct numerical integration.

2.2. Leading Theories for Eccentricity Excitation

Several mechanisms have been proposed to explain the high eccentricities observed in extrasolar planetary systems. The most prominent of these theories are discussed below along with their potential applicability to the υ And system.

Gravitational Perturbation by a Companion Star – Most stars are actually part of a binary or multiple star system. This first theory proposes that in such systems, the planets orbiting one star could be gravitationally perturbed by the companion star, exciting large eccentricities in the planetary orbits. These encounters could induce modulation of eccentricities on long time scales (10^8 years). In fact, the planet orbiting 16 Cyg B has already been shown by Holman, Touma, & Tremaine (1997) to have chaotic variations in eccentricity resulting from such perturbations by a stellar companion. Furthermore, when the relative inclination between the planet and the companion star is $\gtrsim 40°$ and the ratio of the orbital periods is small (around $O(10^{-2})$ to $O(10^{-3})$ (in this case the orbits are called "hierarchical"), the Kozai mechanism can also excite a planet's orbital eccentricity through secular perturbations (Kozai 1962; Takeda & Rasio 2005). Even though the central star of the υ And planetary system does have a stellar companion, perturbations from the companion are dynamically negligible (Chiang & Murray 2002). This theory is also not one of the more appealing in general because only a handful of stars known at present to harbor planetary systems also have stellar companions (see Schneider 2005).

Interactions with a Planetary Disk – For planets having an initial eccentricity exceeding ~ 0.01, Goldriech & Sari (2002) describe how Linblad resonances in the gas disk can excite the planet's eccentricity, in spite of damping effects from corotation resonances. It has also been suggested that convergent migration in a gas disk, a scenario in which the orbit of one planet approaches that of another, can trap two planets into mean motion resonance (meaning the ratio of the orbital periods is near the ratio of two small integers). This subsequently results in pumping of the eccentricities. However, since none of the planets in υ And, nor all but a few planets in any other extrasolar planetary systems, lie in mean motion resonances, this theory also fails to explain the ubiquitously large observed orbital eccentricities among known extrasolar planets. In another scenario involving divergent migration through a gas disk (meaning that the periods of two planets move away from eachother) Chiang, Fischer, & Thommes (2002) discussed how orbital eccentricities are excited by multiple crossings through mean motion resonances. However, they also show that the present configuration of the υ And system does not resemble that of a system in which planets have undergone such resonance crossings. Therefore this scenario cannot explain the large eccentricities of planets c and d.

For the most recent orbital parameters at the time, Chiang and Murray (2002) demonstrated specifically for υ And that eccentricity growth could be accomplished steadily over long time scales ($\gg 10^4$ years) through adiabatic perturbations via torques from an exterior gas disk. For a two planet system, models show that the perturbations from the disk also leave the system in secular resonance by damping the amplitude of libration to zero. This theory is particularly appealing because it is a natural extension of so-called "migration scenarios" for forming hot Jupiters (Ward 1986).

Planet-Planet Scattering – One of the earliest mechanisms proposed to induce large eccentricities in extrasolar planets was planet-planet scattering (Rasio & Ford 1996; Weidenschilling & Marzari 1996). For any system initially consisting of three planets, an impulsive perturbation on the middle planet would arise naturally from a close encounter with the outer planet. The consequential dynamical interactions between the two cause a scattering event in which the outer planet is resultantly ejected from the system. Such a sudden impulsive perturbation imparts a finite eccentricity to the middle planet (Malhotra 2002). Subsequent secular evolution of the system causes the eccentricity of the inner planet in the initial configuration to oscillate between a fairly large value and a value of nearly zero. Secular perturbation theory (Murray & Dermott 1999) predicts the two planets would be left with longitudes of pericenter either circulating or librating with a large amplitude, close to 90°. Applying this scenario to the υ And system, planet c would have been the inner planet, planet d would have been the middle planet, and the outer planet would have been an additional planet that is now lost from the system as a result of the scattering. Because of its small distance from the central star and nearly circular orbit, planet b would play a negligible role.

2.3. Numerical Methods

In all integrations performed for this project, we used a fixed time-step multivariable symplectic (MVS) integrator in the software package `Mercury` (Chambers 1999), version 6.1. The MVS integrator is particularly helpful for our integrations since it is fast for relatively large time steps, while maintaining good energy conservation, $O(10^{-8})$, for essentially regular orbits. The truncation error introduced by symplectic integrators is only that of a Hamiltonian perturbation, and thus the integrator exactly conserves approximate integrals of motion (Chambers 1999).

Planet b is sometimes neglected in numerical integrations simulating resonance the υ And system (see, e.g., Laughlin & Adams 1999). Its proximity to the central star, small eccentricity (most likely a result of tidal circularization), as well as its comparatively large separation from planets c and d, make it much less likely to play a significant role in the evolution of the υ And system. Furthermore, its inclusion can cause integrations to become quite computationally expensive. The short period requires a symplectic integrator to proceed with time steps of only a small fraction of each included planetary orbit in order to prevent energy errors from growing unacceptably large. However, because of the chaotic evolutionary nature of planetary systems, we include planet b in all of our integrations, unless otherwise stated. The time steps used for integrations including planet b are set at 0.5 days, or roughly 10% the period of planet b.

All simulations, unless noted otherwise, are integrated to a maximum of 10^6 years or until the onset of instability occurs, defined here to be a close encounter of two bodies within 0.5 Hill radii (see Gladman 1993). This maximum integration time is unfortunately at least three orders of magnitude below the estimated age of the star (Ford, Rasio, & Sills 1999), on which time scales any systems must be stable if they are to be considered true solutions. However, due to limited computational resources, our maximum integration time was the largest reasonable to allow for a reliable statistical examination of the parameter space allowed by observational data. In §3 we show that truncating integrations after 10^6 years most likely does not cause in a significant number of systems to be incorrectly identified as solutions.

Stopping the integrations after the first close encounter between two bodies prevented energy errors due to the fixed time step of the MVS integrator from becoming unacceptably large. Close encounters in a multiple planet system are also generally reliable indicators that the system will eventually become unstable, as indicated by one of three events: the collision of two planets, the collision of a planet with the central star, or the ejection of a planet from the system. However, even after close encounter, there is still no guarantee as to how long it will take for one of these events to occur.

2.4. Initial Conditions

We model the observations as resulting from three planets on independent Keplerian orbits. We use a Bayesian framework (Gelman et al. 2003) to constrain the orbital elements and masses with the radial velocity observations, as well as the "stellar jitter" (radial velocity variations due to stellar phenomena such as convection, star spots, and rotation). We assume priors uniform in the logarithms of orbital periods, velocity semi-amplitudes, and the stellar jitter. We assume uniform priors for the eccentricities and the remaining angles. The effects of stellar oblateness and general relativistic precession were neglected.

We use the techniques of Markov chain Monte Carlo (MCMC) and the Metropolis-Hastings algorithm with the Gibbs sampler to sample from the posterior probability distribution for the masses and orbital parameters (Ford 2005). Our Bayesian analysis closely follows the methods developed for single-planet systems with no stellar jitter by Ford (2005), here we only discuss the generalizations to the algorithm that were necessary to apply it to multiple-planet systems and allow for an unknown stellar jitter. Each state of the Markov chain includes five fit parameters for each planet (orbital period, P, velocity semi-amplitude, K, orbital eccentricity, e, argument of pericenter, ω, and mean anomaly at the specified epoch, M_o), the unperturbed stellar velocity, C, and the magnitude of the stellar jitter, σ_j. The jitter is assumed to be Gaussian candidate transition functions, which are centered on the parameter values from the current state in the Markov chain. The scales of the candidate transition functions were chosen based on a preliminary Markov chain so as to result in acceptance rates of nearly 40%. The computational efficiency of MCMC can also be significantly affected by correlations between variables. To improve the computational efficiency we added candidate transition functions, which were based on several auxiliary variables based on combinations of the fit parameters. These auxiliary variables are $e\sin\omega$, $e\cos\omega$, $\omega+M_o$, $\omega-M_o$, $P^{2/3}(1+e)$, and $P^{2/3}(1-e)$, for each planet, as well as $\omega_b\pm\omega_c$, and $\omega_c\pm\omega_d$ (where ω_b, ω_c, and ω_d are the arguments of pericenter for planets b, c, and d, respectively). The acceptance ratio was deterimined according to the Metropolis-Hastings algorithm to reflect our choice of priors described in the previous paragraph. The use of this enlarged set of candidate transition functions significantly improved the mixing and hence efficiency of our Markov chains. It is important to note that our sampling procedure does not make any assumptions about the posterior distribution for the orbital elements or masses. Therefore, our approach allows us to take into account correlations between various orbital parameters, in contrast to previous simpler analyzes.

We have computed five Markov chains, each of which contains over one million states. We have performed several checks to verify the reliability of our Markov chains. The acceptance rates were between 0.37 and 0.45 for trial stages generated by the candidate transition functions for each auxiliary variable in each chain. We have also verified that the resulting distributions show excellent agreement across all five chains. For example, the Gelman-Rubin test statistic, $\hat{R}$, approaches 1 from above as a Markov chain approaches convergence. While sets of Markov chains with $\hat{R}$ less than 1.1, or even 1.2, are frequently used for inference, for the Markov chains used in this analysis, $\hat{R}$ was less than 1.001 for each fit parameter and auxiliary variable, and for the predictions of the radial velocity at 40 future epochs. Thus we are very confident in the reliability of our Markov chains.

The results from them form the basis for our dynamical analyzes. When considering non-coplanar cases, we independently drew the inclinations from isotropic distributions and the longitude of ascending node from a uniform distribution. For each state in the Markov chain, we calculate the planet masses and semimajor axes iteratively and treat them as Jacobi elements. Finally, we have performed more than 7000 direct N-body integrations of systems sampled from our Markov chains in order to thoroughly investigate the allowed parameter space. For these integrations, we chose a variety of initial epochs varying by several times the orbital period of planet d. By comparing the χ^2 of the fit determined by the analytic and N-body models, we have determined that our results are not affected by including the effects of mutual planetary perturbations in the fitting procedure. The N-body numerical integrations were done in sets of 1000; for each set the unknown inclination angles, i and Ω, were varied randomly within specific ranges. Table 4 lists specifications of i and Ω, along with the some of the results (discussed further in the next section) for each set of 1000 integrations.

3. Results

3.1. Constraining Inclinations from Stability Requirements

In order for the system to remain stable over the full 10^6 year integration, we find that the inclination with respect to the line of sight, i, must be $\lesssim 30°$. This implies that the masses for a coplanar system must be no more than about twice their minimum value, since $m = m_{obs}/\sin(30°) = 2 \times m_{obs}$.

Systems are usually unstable for relative inclinations $\gtrsim 40°$. Note that systems with relative inclinations $\geq 140°$ are also dynamically stable. Although, such retrograde orbits are unlikely on theoretical grounds, our conclusions are robust to this possibility. (Since it averages over the orbits, secular perturbation theory is also valid for retrograde orbits.) Interestingly this value is close to the Kozai angle (Kozai 1962). However, because the orbits of planets c and d are not hierarchical, the periods are in fact comparable, the perturbative Kozai mechanism is not likely to be so relevant in this system.

In Figure 1 we show a histogram of the time to first close encounter t_{ce}, for two sets of 1000 integrations, where the initial angles of inclination were determined randomly, with the only other constraint on the data in the lower panel that the relative inclinations between υ And c and d were $\leq 30°$ (these correspond to set #7 in the top panel and set #6 in the lower panel as described in Table 4). Since t_{ce} was between 10^3 and 10^5 years for about 85% of integrations in both panels, the integration time appears to be sufficient to find a majority of systems that will go unstable on timescales $\gtrsim 10^6$ years. If systems became unstable at a high rate beyond integration times of $\gtrsim 10^6$ years, we would expect to see an upward trend in the percentage of systems that go unstable as integration time increases.

3.2. Evidence for Planet-Planet Scattering

Throughout the full range of allowed inclination angles we find qualitatively similar behavior for the secular evolution of the system.

There is less correlation between secular resonance and stability in our results than in some previous studies (see discussion in §1.2.4). Table 4 shows the total number of librating, circulating, and unstable systems according to the initial conditions for each set of 1000 integrations. For the coplanar, edge on simulations, roughly half are found to be librating and half are found to be circulating. Among stable configurations in each set of integrations the number of systems found to be librating and circulating are usually comparable.

The evolution over secular timescales of the coplanar, edge-on system for the current best-fit orbital parameters is shown in Figure 2. The eccentricity of planet d remains always between 0.25 and 0.35. While the eccentricity of planet c is large at present time (t = 0), note that it returns periodically to a nearly circular orbit with $e_c < 0.01$, roughly every 6700 years.

In many systems it appears that the longitudes of pericenter for planets c and d are “switching” between librating and circulating, which is a phenomenon not documented in previous studies. However, it is not clear if these systems are truly switching in and out of librating configurations. For these systems the maximum separation of longitudes of pericenter, i.e. $|\varpi_c - \varpi_d|$, often occurs when the eccentricity of planet c is near its minimum; a representative example is shown in Figure 3. When its eccentricity is very nearly zero, the orbit of planet c is almost circular causing the position of the pericenter to become less well-defined than for larger eccentricities. Because the data loses some of its physical significance at times of near zero eccentricity, it is difficult to determine whether planets c and d are actually in a librating configuration. Fortunately, we did not find a large number of such ambiguous systems in proportion to the total number of integrations. Thus for our purposes, librating systems were defined to be any for which the maximum change in separation of longitudes of pericenter, $\Delta|\varpi_c - \varpi_d|$, never exceeded 240° from one data point to the next; otherwise the system was classified as circulating.

Small minimum eccentricities are a property of all solutions consistent with the observational data, as opposed to suggestions previously that this was a characteristic only of some solutions (Lissauer & Rivera 2001). In Figure 4 we have determinded the probability distribution for the minimum eccentricity of planet c for both coplanar, edge-on systems and for orbits with random orientations to the line of sight, but requiring dynamical stability; this implies relative inclinations $\leq 40°$. This result can be understood from lowest-order secular perturbation theory (Malhotra 2002; Murray & Dermott 1999), where the eccentricity vector of each planet can be described as the sum of three rotating eigenvectors in the $(e \cos \omega,\, e \sin \omega)$ plane. The eigenvector representing the effects of planet b on planet c has a very small amplitude and thus can be neglected. For the particular configuration of υ And , the two dominant eigenvectors describing planet c have very nearly the same length. If the eigenvector with the faster rotation (in other words, the eigenvector with the higher eigenfrequency) has a slightly larger length than the other, the vector sum will be rotating around 360°, indicating that the longitudes of pericenter for planets c and d are circulating. Instead, if the eigenvector with the faster rotation has a slightly smaller length than the other, the vector sum will be oscillating with an amplitude close to 90°, corresponding to secular resonance between planets c and d. Whenever the two vectors are anti-aligned, the magnitude of their sum, which is equal to the eccentricity of the planet, is very close to zero; when they are aligned, the eccentricity is maximum.

Our numerical integrations also suggest that the allowed solutions all lie very close to the boundary between librating and circulating configurations (see Figure 5). Indeed, the division between librating (triangles) and cirulating (squares) system in the figure falls within the 1-σ uncertainties for the separatrix derived from the classical second-order secular perturbation theory, when planet b is neglected. As a consequence of the proximity of this observed planetary configuration to the separatrix, all librating systems have large libration amplitudes, as shown by Figure 6. The median libration amplitude is close to 80°. This result may also help to explain why the presence of secular resonance in the υ And system has been such a long-standing controversy. Clearly if the best-fit parameters had fallen slightly to the left or to the right of the current measurements, the system would have appeared to be almost entirely to one side of the separatrix. Subsequent numerical integrations would suggest that either most solutions exhibit evidence of libration, or that most solutions have the pericenters of planets c and d circulating, according to the side of the separatrix on which the observations had placed the best-fit parameters.

3.3. Scattering Models

Our analysis clearly confirms that the υ And system is evolving exactly as would be expected after an impulsive perturbation to planet d (Malhotra 200). The initial sudden change in eccentricity for planet d would naturally be produced by a close encounter with another planet that got ejected from the system as a result.

3.3.1. One Additional Planet

Using our knowledge of planet-planet scattering from several previous studies (e.g. Rasio & Ford 1996; Ford, Havlickova, & Rasio 2001), we have determined plausible initial conditions for the original, unstable system. We have adopted a simple two-planet configuration for computational convenience in which two planets on circular orbits perturb eachother significantly, with the other planets distant enough to be negligible.

The early dynamical evolution of such a system including one additional planet (for clarity we refer to the extra planet as "planet e") set initally beyond the orbit of planet d, is illustrated in Figure 7. Planet b was not included, since it plays an insignificant role. All planets were set on nearly circular orbits at the start of the integration. The initial periods of planets c, d, and e were 241.5 days (equal to the present period of planet c), 2100 days and 3333 days. The masses of planets c and d were set at their current observed minima, and the mass of planet e was set at $1.9 M_J$ so that planets d and e were near their dynamical stability limit, which is known and sharply defined (Gladman 1993).

As shown in Figure 7, planet e interacted strongly with planet d for a brief period lasting $\sim 10^3$ years, while planet c maintained a small eccentricity. After the ejection, the remaining two planets are left in a dynamical configuration closely resembling that of the υ And system as it is observed at present (cf. Figure 2). Note that the timescale to completely eject planet e from the system ($\sim$ 9000 years in this particular simulation) is much longer than the timescale of the initial strong scattering. After the brief period of strong interaction, the perturbations on the outer planet are too weak to affect significantly the coupled secular evolution of planets c and d. Thus the "initial" eccentricity of planet c for the secular evolution is determined by its value at the end of the strong interaction phase, rather than at the time of the final ejection.

3.3.2. Two Additional Planets

We performed a total of 1500 integrations where two additional planets, "planet e" and "planet f" in order of increasing distance from the central star, were placed outside the initial orbit of planet d. Seven hundred of these integrations were set so that planets d and e were near the dynamical stability limit (case 1), and seven hundred were set so that planets e and f were near the dynamical stability limit (case 2), with the remaining two planets sufficiently far from all the other planets so as to be negligible. One hundred more integrations were performed with planets e and f farther outside of the dynamical stability limits for all included planets (case 3).

With the addition of two planets to systems already including planets c and d, we see a more chaotic evolution than with only one additional planet, as expected. For systems in case 1, we originally anticipated that planets d and e would perturb eachother strongly, but the gravitational force of planet f on e would help to remove planet e quickly from the vicinity of planet d after imparting a finite eccentricity to it. In case 2, we expected a similar scenario where mutual perturbations between planets e and f result in a short period of strong interaction between one of these two outer planets and planet d. Eventually in either case, planet e or f would be ejected from the system, leaving planets c and d in their presently observed configurations. The initial conditions for the systems in case 3 are the most natural since each pair of adjacent planets is farther from their stability limits. However, for this reason case 3 is also the least efficient in producing scattering events because it is less clear how long it may take for strong gravitational interactions to develop between any pair of planets, if they develop at all.

For case 1, our results show, contrary to our expection, that while either planet e or f was ejected from the system in 326 of the 700 simulations, planets c and d both survived the full 10^6 year integration in only 24 of them; no systems were found to be stable. For case 2, 304 systems resulted in the eventual ejection of either planet e or f, but planets c and d survived in just 19 of these, while 31 systems remained stable. Case 3 yeilded 14 systems for which either planet e or f was ejected, but only 3 systems in which planets c and d survived. Since all planets began on orbits more stable than the previous two cases, a larger fraction, 62 out of 100, remained stable for 10^6 years.

In Figure 8 we show the secular evolution of one of the 3 systems from case 3 in which planet e was ejected, and planets c and d survived. For this specific system, the initial semimajor axes for planets c and d were 0.91 AU and 4.59 AU, respectively. Planet e was given a mass of $6.93M_J$ and an initial semimajor axis of 8.84 AU; planet f was given a mass of $17.35M_J$ and began the integration with a semimajor axis of 15.31 AU. This simulation is an excellent example of the manner in which a scattering event may occur in a multiple-planet system. After more than 800,000 years of seemingly stable and regular evolution, planets e and f suddenly begin to perturb eachother strongly. In the course of their interaction, planet e was flung farther out into the system while planet f moved in closer to the central star, at which time it perturbed planet d very quickly and continued to interact strongly exclusively with planet e afterward, until planet e was eventually ejected from the system. From the point at which the eccentricity and the semimajor axes of the planets began to evolve erratically, indicating the onset of instability in the system, to the time that planet e was ejected spans only $\sim 15,000$ years.

In about half of the 46 simulations for all 3 cases in which either planet e or f was ejected and planets c and d both survived, we find often that by the end of the integration, planets f and d have switched positions; in other words, planet d became the farthest of the three remaining planets (almost always with a semimajor axis exceeding 15 AU) and planet f became the second farthest out (with a semimajor axis of $\sim 3-5$ AU, about that of the second planet from the central star in the υ And system as it is observed at present). Thus, future work will include a more thorough examination of the systems in which planets c or d did not survive, in order to determine the frequency with which two planets switch positions after a scattering event and leave the system in a configuration resembling closely that of υ And today.

Reproducing the exact parameters of any particular observed system always requires "fine tuning" in an obvious sense. What is important here is that our mechanism can naturally, without any fine tuning, provide the very short timescale required for the initial perturbation that left planet d on an eccentric orbit and planet c on an almost perfectly circular orbit.

4. Summary and Discussion

By requiring that orbital configurations of the υ And planetary system remain stable for at least 10^6 years, we were able to constrain the relative inclination, i_{rel}, as well as the unknown angle of inclination with respect to the plane of the sky, i. For the best-fit orbital parameters in the coplanar case, the system is unstable when $i \gtrsim 30°$. From this result, we can conclude that the masses of the planets must be no more than twice the observed minimum masses. The maximum allowed relative inclination between each pair of planets is $\sim 40°$.

According to the most recent best-fit parameters allowed solutions lie close to and on either side of the theoretical separatrix between circulating and librating systems. The approximate dividing line between circulating and librating systems from our numerical integrations does in fact lie within the 1-σ errors of this separtrix. This may explain the reason previous studies of this system had difficulty establishing whether planets c and d are in a resonant, librating, or circulating configuration.

Dynamical instabilities between two planets set close to each other on initially circular orbits have previously been found to produce the kinds of unexpectedly large eccentricities observed in extrasolar planetary systems. Usually when one planet is ejected, the other planet is left on a highly eccentric orbit (Rasio & Ford 1996; Weidenschilling & Marzari 2001). However, these close encounters also produce a significant number of collisions, causing the resultant planet to trace a nearly circular orbit, which are not proportionally represented in the observed data (Ford, Havlickova, & Rasio 2001). The results presented here provide evidence nonetheless that dynamical interactions must have resulted in the instability that caused a scattering event to take place in the υ And system. Our results therefore imply that the evolutionary history of the system very well may be common, and thus explain why extrasolar planets are so often observed to have large eccentricities. More work must be done to determine how collisions might be avoided (Ford, Rasio, & Yu 2003).

While the simulation in Figure 7 illustrates a case in which υ And had only one extra planet, our results do not preclude the existence of even more planets at larger distances. In fact, the presence of another planet in an even longer-period orbit could be responsible for triggering the instability after a long period of seemingly "stable" evolution and help raise more quickly the pericenter of planet e, similar to the simulation shown in Figure 8. Although equally plausible, this is less computationally convenient since, with more than two planets, the stability limit is not known analytically and not sharply defined, so numerical experimentation would be needed to find a case that could produce a final state resembling the current configuration of υ And , possibly after a very long dynamical integration. The secular evolution of the system should be reevaluated if future observations of υ And were to discover an additional planet in a long period orbit.

As discussed in previous papers, a variety of scenarios would naturally lead to two planets approaching their dynamical stability limit (Rasio & Ford 1996; Ford, Havlickova, & Rasio 2001). For example, planet e might be migrating inward through coupling with an outer gaseous disk. Once the stability limit is reached, the system evolves quickly (on the orbital timescale) until strong scattering occurs and one planet is ejected, while the gas becomes irrelevent (as the viscous timescale is much longer). Furthermore, with more than two planets added beyond the orbit of planet d, the timescale for growth of the instability and the occurrence of a strong scattering can be arbitrarily long (Gladman 1993; Chambers 1996) and could easily exceed the 10^7 year timescale on which the gas is expected to be lost from the protoplanetary disk. If gas were still present when the scattering occurs, the final outcome would be modified, but only the details of the dynamical evolution would change. For example, if gas drag produces some damping effect on the eccentricity, then a slightly stronger scattering may be needed to produce the same final eccentricity for the retained planet.

Several mechanisms other than scattering, such as perturbation by a binary star (Holman, Touma, & Tremaine 1997) and interaction with a gaseous disk (Goldreich & Sari 2003), have been proposed to explain the large eccentricities of extrasolar planets. However, only planet-planet scattering naturally results in an impulsive perturbation, as is necessary to explain the current orbital configuration of the υ And system. All other mechanisms operate on much longer timescales and would also affect the eccentricity of planet c, erasing the memory of its initial circular orbit.

Specifically, the possibility that the impulsive perturbation to planet d was delivered by a massive exterior gaseous disk with a large viscosity was mentioned in a previous study (Malhotra 2002). However, we can now show that this possibility is firmly excluded from this system. If the eccentricity of planet d had been induced by an outer disk, the eccentricity growth time would have to be considerably shorter than the secular timescale. In addition, after the eccentricity grew to ~ 0.3, the perturbation must stop suddenly; otherwise the eccentricity of the middle planet, planet c, would also start growing and its "initial" value would no longer be compatible with the minimum we derive in the secular solution.

Quantitatively, this is a very stringent requirement. We have performed additional numerical integrations for the outer two planets, starting with their current masses and orbital periods, but on circular orbits. In addition to the mutual gravitational perturbations, we include a simple semi-analytic model of angular momentum dissipation acting on planet d only. The dissipation rate, $\dot{J}$, is constant for a time Δt and then disappears (completely and instantaneously). We have performed multiple simulations holding the product $\dot{J}\Delta t$ fixed to reproduce the current eccentricity of planet d. If we impose the constraint that the eccentricity of planet c must remain $\lesssim 0.01$ (the current best-fit value of the minimum is 0.005) after Δt, then this model provides an upper limit of $\Delta t \lesssim 100$ years.

A timescale for eccentricity growth by viscous coupling to a disk as short as $\lesssim 100$ years would require both an implausibly massive disk and a very high effective viscosity. The possibility of eccentricity growth caused by interactions with a disk is rather controversial (Papalouizou, Nelson, & Masset 2001), particularly for planets less massive than $10 - 20 M_J$. Nevertheless, we have estimated the timescale for eccentricity using the only detailed theory of eccentricity excitation by viscous coupling to a disk in the astrophysical literature (Goldreich & Sari 2003). We find that a timescale for eccentricity growth as short as ~ 100 years would require a mass in the relevant part of the disk, $\Sigma r^2 \sim 40 M_J$, ten times more than the mass of the planet, even with an implausibly large disk viscosity parameter, $\alpha \sim 0.1$. Instead, using more typical parameters (Goldreich & Sari 2003) (for a $1 M_J$ planet at 1 AU, with disk parameters $r/h = 25$, $\alpha = 0.001$, and $w/r = 0.5$), it would require $\sim 10^7$ years for the eccentricity to grow from 0.01 to 0.3. Eccentricity growth on this very long timescale would instead lead to secular resonance between planets c and d with a small amplitude libration (Chiang & Murray 2002), which our results rule out. In addition, neither this theory (Goldreich & Sari 2003) nor any other published theory of eccentricity excitation due to a gas disk provides a mechanism for making the perturbation cease quickly ($\lesssim 100$ years) after a phase of very rapid eccentricity growth.

Planet-planet scattering is truly unique in that it provides both a very short timescale for eccentricity growth (the dynamical timescale on which the instability develops) and the same very short timescale for removing the perturbation, since the extra planet is ejected as a result of the scattering.

These results have additional implications for planet formation as well. Given the difficulty of forming giant planets at small orbital distances, it is generally assumed that the planets in the υ And system followed the standard picture of orbital evolution (Lin D.N.C. 2000) and migrated inward to their current locations via interactions with the protoplanetary disk. If this is correct, then the small minimum eccentricity of υ And c also provides evidence that its eccentricity at the end of migration had not grown significantly, in contrast to the theory suggesting eccentricity excitation through torques applied by the gaseous disk (Goldreich & Sari 2003). However, the possibility that the planets did in fact form near their current positions as described in Bodenheimer, Hubickyj, & Lissauer (2000) rather than undergoing migration through a disk cannot be excluded by our results.

I am immensely grateful for the extensive support and guidance of my advisor, Professor Frederic Rasio. I would like to acknowledge the gracious help of Dr. Eric Ford, who along with Professor Rasio made this project possible. Much thanks to Debra Fischer for providing the updated radial velocity data for the υ And planetary system. I would also like to acknowledge support from the NASA Undergraduate Summer Research Program at Northwestern University through the Illinois Space Grant Consortium, as well as the NSF Research Experiences for Undergraduates program.

REFERENCES

Barnes, R. & Quinn, T. 2001, ApJ, 550, 884

Bodenheimer, P., Hubickyj, O., & Lissauer, J.J. 2000, Icarus, 143, 2

Boss, A.P. 1995, Nature, 377, 578

Butler, R.P., Marcy, G.W., Fischer, D.A., Brown, T.W., Contos, A.R., Korzennik, S.G., Nisenson, P., & Noyes, R.W. 1999, ApJ, 526, 916

Chambers, J.E. 1999, MNRAS, 304, 793

Chiang, E.I. & Murray, N. 2002, ApJ, 576, 473

Chiang, E.I., Tabachnik, S., & Tremaine, S. 2001, AJ, 122, 1607

Fischer, D.A., Marcy, G.W., Butler, R.P., Vogt, S.S., Henry, G.W., Pourbaix, D., Walp, B., Misch, A.A., Wright, J.T. 2003, ApJ, 586, 1394

Ford, E.B. 2005, AJ, 129, 1706

Ford, E.B., Havlickova, M., & Rasio, F.A. 2001, Icarus, 150, 303

Ford, E.B., Rasio, F.A., & Sills, A. 1999, ApJ, 514, 411

Gelman, A., Carlin, J.B., Stern, H.S. & Rubin, D.B. 2003, *Bayesian Data Analysis.* Chapman & Hall/CRC (New York)

Gladman, B. 1993, Icarus, 106, 247

Goldreich, P. & Sari, R. 2003, ApJ, 585, 1024

Hill, G.W. 1878, *Am. J. Math*, 1, 5, 129, 245

Kozai, Y. 1962, AJ, 67, 591

Laughlin, G. & Adams, F.C. 1999, ApJ, 526, 881

Laughlin, G. & Chambers, J.E. 2001, ApJ, 551, L109

Lin, D.N.C. *et al.* in *Protostars and Planets IV* (eds Mannings, V., Boss, A.P., & Russell, S.S.) 1111-1178, University of Arizona Press, Tucson (2000)

Lin, D.N.C. & Ida, S. 1997, ApJ, 477, 781

Lissauer, J.J. & Rivera, E.J. 2001, ApJ, 554, 1141

Lowrance, P.J., Kirkpatrick, J.D., & Beichman, C.A. 2002, ApJ, 572, L79

Marzari, F. & Weidenschilling, S.J. Icarus, 156, 570

Mayor, M. & Queloz, D. 1995, Nature, 378, 355

Mazeh, T., Zucker, S., Dalla Torre, A., & Van Leeuwen, F. 1999, ApJ, 522, L149

Murray, C.D. & Dermott, S.F. 1999, *Solar System Dynamics.* Cambridge University Press (New York)

Pollack, J., Hubickyj, O., Bodenheimer, P., Lissauer, J., Podolak, M., & Greenzweig, Y. 1996, Icarus, 124, 62

Rasio, F.A., Tout, C.A., Lubow, S.H., & Livio, M. 1996, ApJ, 470, 1187

Rasio, F.A. & Ford, E.B. 1996, Science, 274, 954

Schneider, J. Extrasolar planets catalog. May 2005 (http://cfa-www.harvard.edu/planets/catalog.html)

Stepinski, T.F., Malhotra, R., & Black, D.C. 2000, ApJ, 545, 1044

Takeda, G. & Rasio, F.A. 2005, ApJ, in press (`astro-ph/0502404`)

Ward, W.R. 1986, Icarus, 67, 164

Weidenschilling, S.J. & Marzari, F. Nature, 384, 619

This preprint was prepared with the AAS LaTeX macros v5.2.

Table 1. Orbital Elements

Symbol	Name	Description
a	semimajor axis	half the length of the longest distance between two points of the orbital ellipse
b	semiminor axis	half the length of the shortest distance between two points of the orbital ellipse
e	eccentricity	equal to $\sqrt{1-(b/a)^2}$ where a and b are the semimajor and semiminor axes of the orbital ellipse; thus $e=0$ corresponds to a perfect circle, while $e=1$ corresponds to a straight line
f	true anomaly	the angle between the line from the central star to the pericenter and the line from the central star to the planet
i	inclination	the angle between the plane of the orbit and a reference plane
ω	argument of pericenter	the angle between the line from the central star to the longitude of ascending node and the line from the central star to the pericenter
Ω	longitude of ascending node	the angle between the line from the central star to a reference direction and the line from the central star to the point on the orbit where the planet crosses from below the reference plane to above the reference plane
ϖ	longitude of pericenter	equal to $\omega+\Omega$; note that this is a "dogleg" angle since ω lies in the orbital plane and Ω lies in the reference plane
$T_{\rm peri}$	time of pericenter passage	the time at which the planet passes through the point on its orbit closest to the central star

Table 2. Up-to-Date Orbital Elements for the υ And Planetary System

Planet	P(d)	e	ω(deg)	$m \sin i (M_J)$
b	4.617146(56)	0.016(11)		0.6777(79)
c	241.32(18)	0.258(15)	250.2(4.0)	1.943(35)
d	1301.0(7.0)	0.279(22)	287.9(4.8)	3.943(57)

Note. — Results of our new analysis of the υ And radial velocity data (Ford 2005). We have used the entire Lick Observatory data set, kindly provided to us by D. Fischer. For conciseness, we present only the means and standard deviations on the last two digits (indicated in parenthesis) after marginalizing over all other parameters. We list the orbital period (P) in days, the orbital eccentricity (e), the argument of pericenter (ω) in degrees, and the planet mass times the sine of the inclination of the orbital plane to the line of sight ($m \sin i$) in units of Jupiter masses (M_J). The argument of pericenter for planet b is omitted because its orbit is nearly circular and thus the exact position of the pericenter is not only difficult to identify within a meaningful confidence interval, but also it loses physical significance in this limit.

Table 3. 2003 Orbital Elements for the υ And Planetary System

Planet	P(d)	e	ω(deg)	$m \sin i (M_J)$
b	4.6171(01)	0.019(02)		0.71
c	241.2(0.5)	0.26(03)	249.1(9.3)	1.98
d	1283(12)	0.25(03)	264(18)	3.9

Note. — Previously most recent orbital parameters for the υ And system from Fischer et al. 2003. As in Table 1, for ease of comparison we list the orbital period (P) in days, the orbital eccentricity (e), the argument of pericenter (ω) in degrees, and the planet mass times the sine of the inclination of the orbital plane to the line of sight ($m \sin i$) in units of Jupiter masses (M_J).

Table 4. Inclination and Results for Sets of 1000 Integrations

Set #	$i_{\max}$ (deg)	$i_{\min}$ (deg)	$\lvert i_c - i_d \rvert$ (deg)	$\Omega_c - \Omega_d$ (deg)	Librating	Circulating	Unstable
1	90	90	0	0	580	420	0
2	11.5	168.5	0	0	372	409	219
3	90	90	0	random	48	173	779
4	82.5	97.5	0	random	34	173	793
5	60	120	0	random	63	134	803
6	random	random	≤ 30[a]	random	82	365	553
7	random	random	random	random	7	53	940

[a]Indicates the range in relative inclinations $i_{\rm rel,cd}$, not separation of angles of inclination with respect to the line of sight $\lvert i_c - i_d \rvert$ for this set only.

Note. — Inclination specifications and results for sets of 1000 N-body numerical integrations. The maximum and minimum inclinations with respect to the line of sight, $i_{\max}$ and $i_{\min}$ respectively, specify the range for initial values, and are given in degrees. The separation between i_c and i_d, which are given in the next column in degrees. It is important to remember that this separation is indicative of differences in actual masses and not equal to the relative inclination between the planets, $i_{\rm rel,cd} = \cos i_c \cos i_d + \sin i_c \sin i_d \cos(\Omega_c - \Omega_d)$. Only the values of i affect the actual planetary masses used in the integration; Ω plays a role in the relative inclination of the orbits, but has no bearing on the true masses, since the observed mass is $m \sin i$. Angles that are stated as "random" are generated randomly to be within the range of $-180°$ to $180°$. The last three columns indicate how many systems out of the total 1000 integrated for the set were found to be either stable and librating ("Librating"), stable and circulating ("Circulating"), or unstable, indicated by a close encounter of two bodies to within 0.5 Hill radii, before the termination of the integration at 10^6 years ("Unstable").

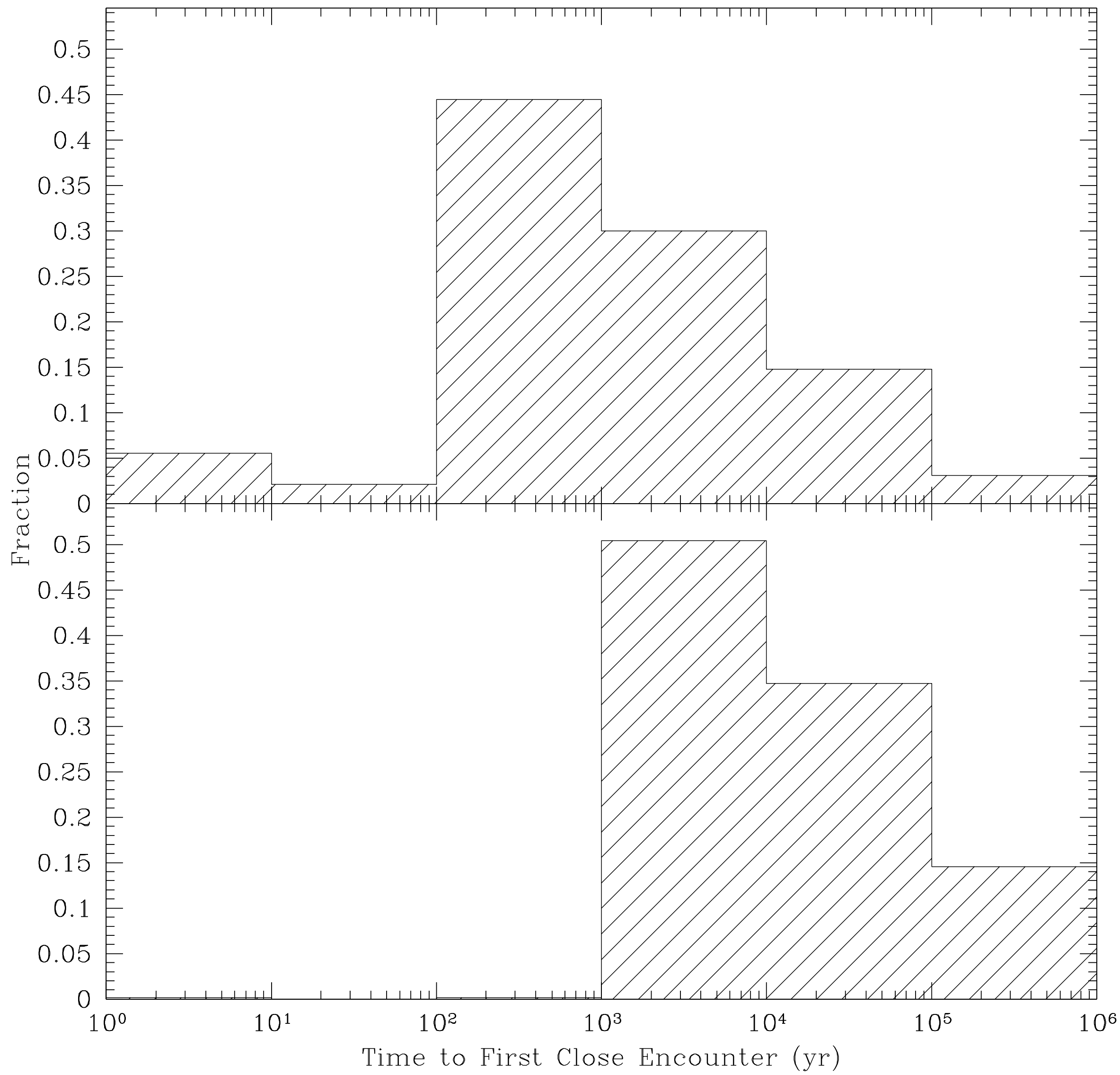

Fig. 1.— Histogram of time to first close encounter. The data used for the top panel was taken from the 1000 integrations of sets #7 in Table 3, where angles of inclination, i and Ω are chosen randomly between $-180°$ and $180°$ for both planets c and d. The data for the bottom panel was taken from the 1000 integrations of set #6 in Table 3 where the angles of inclination were chosen randomly with the only addtional requirement that $i_{\rm rel,cd} = \cos i_c \cos i_d + \sin i_c \sin i_d \cos(\Omega_c - \Omega_d) \leq 30°$.

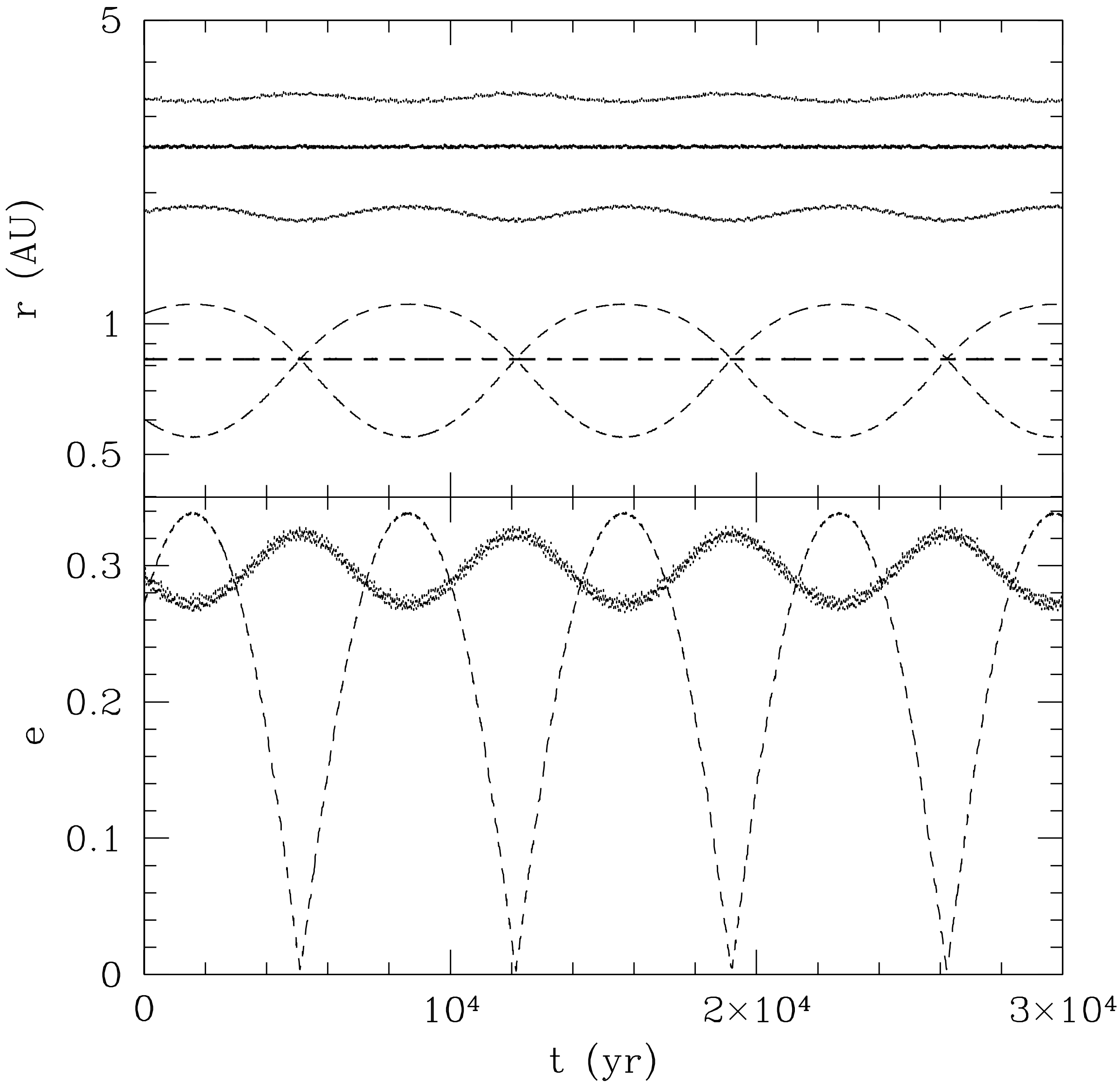

Fig. 2.— Secular evolution of the triple-planet system around υ And. The top panel shows the semimajor axes (middle lines), as well as the pericenter and apocenter distances (lower and upper lines respectively) for the outer two planets. The lower panel shows the evolution of the orbital eccentricity for each planet. Note that both υ And c (dashed) and υ And d (dotted) have a signficant eccentricity at the present time ($t = 0$), but that the eccentricity of c returns periodically to very small values near zero. The results shown here were obtained by direct numerical integration using the best-fit parameters.

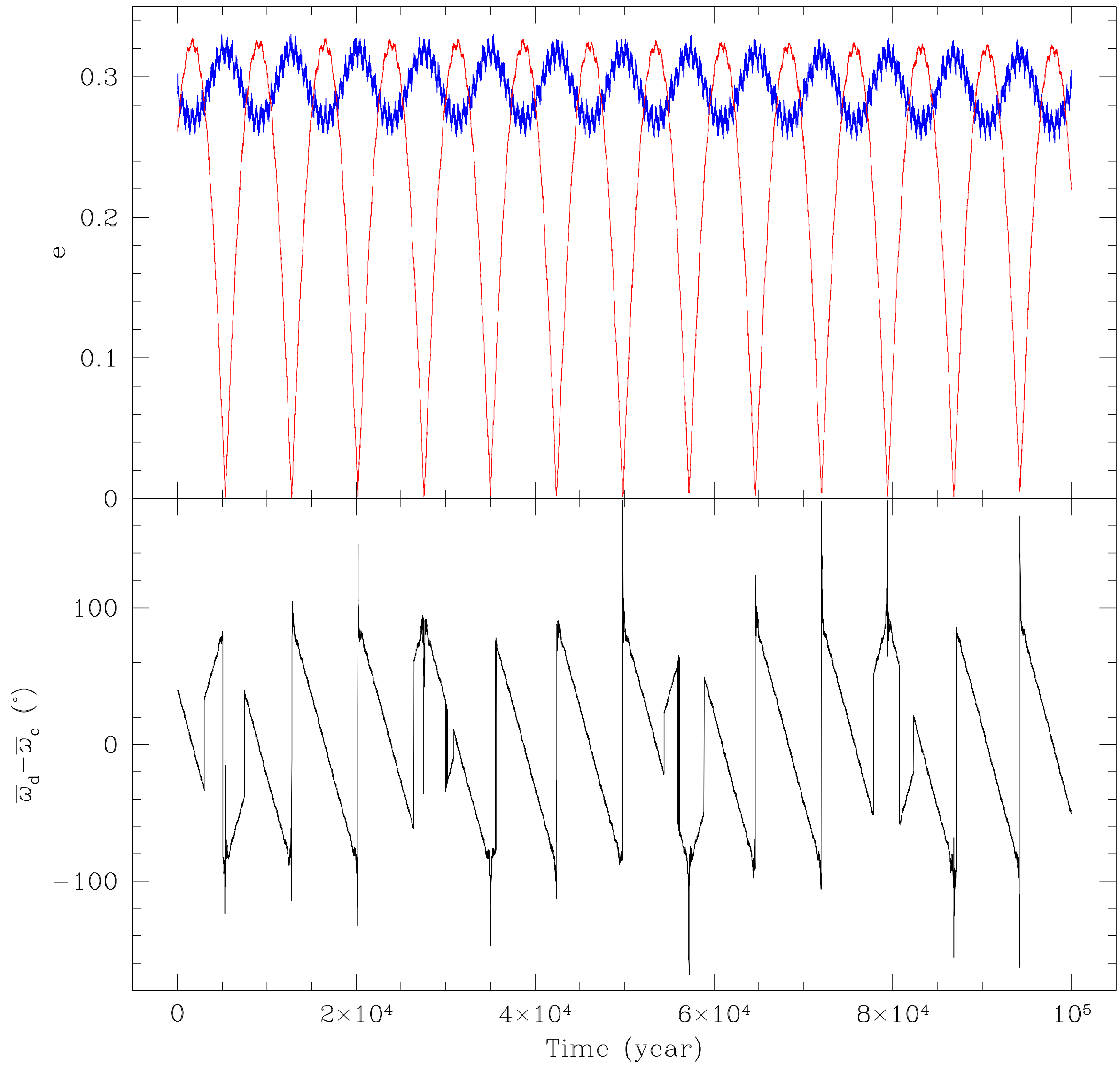

Fig. 3.— Top panel: Eccentricity versus time for υ And c (upper curve) and υ And d (lower curve). Bottom panel: Separation between longitudes of pericenter for υ And c and υ And d versus time. For the coplanar, edge-on (minimum masses) case, several systems that seemed to exhibit libration at fairly large amplitudes, generally near 90°, initially appeared to be switching between librating and circulating configurations. However, large excursions in the separation of longitudes of pericenters can be explained by υ And c's periodic return to eccentricities extremely close to zero, which causes the location of the pericenter to be less well-defined.

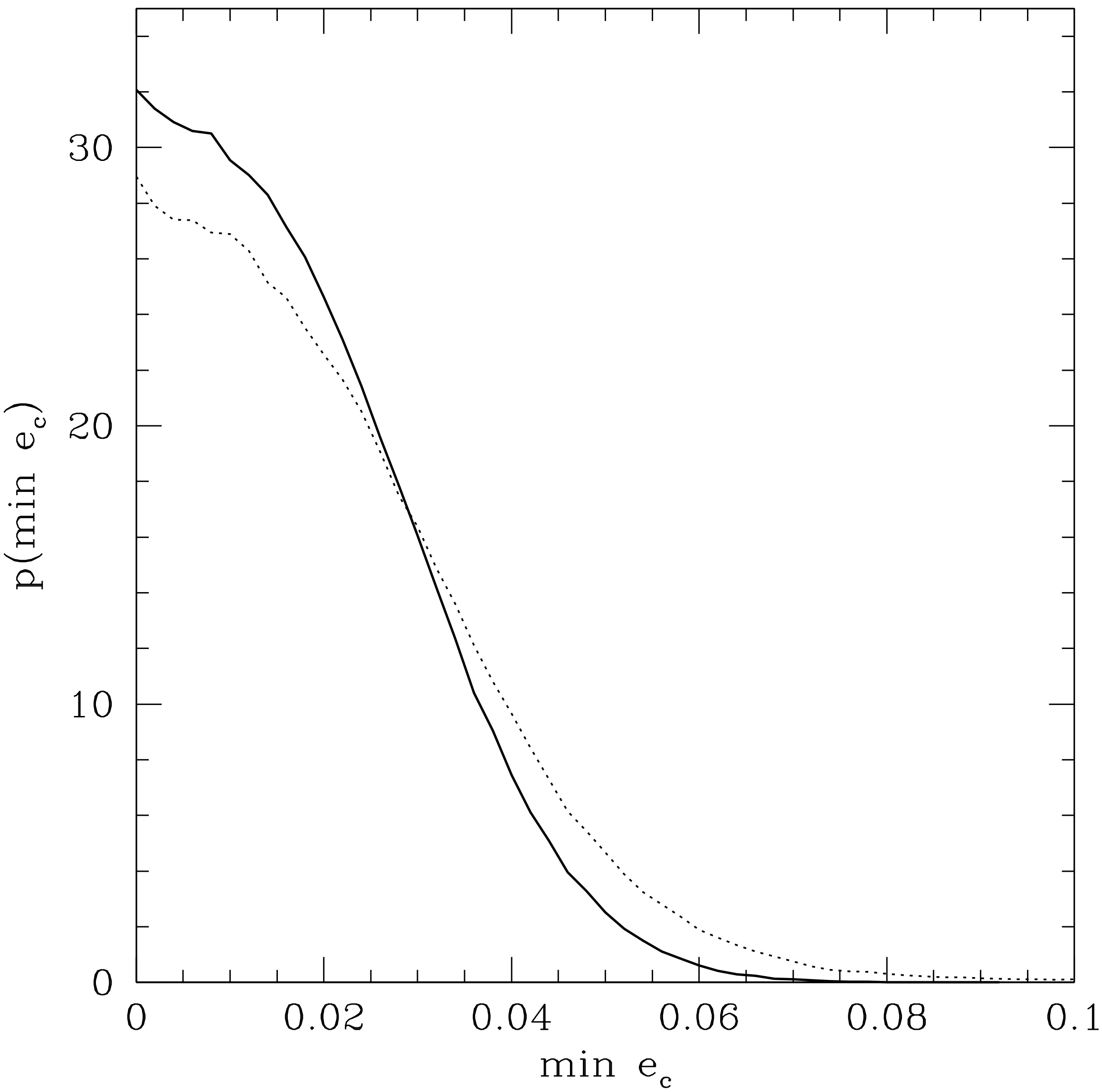

Fig. 4.— Probability distribution for minimum eccentricity of planet c. We draw initial orbital elements for planets b, c, and d from their posterior probability distribution and evolve each system according to classical second-order secular perturbation theory. We find that all allowed orbital solutions have the eccentricity of planet c oscillating from a maximum value slightly larger than the present value to very nearly zero. The solid curve corresponds to coplanar orbits viewed edge-on. The dotted curve shows the result for orbits with random orientations to the line of sight, but requiring dynamical stability. This implies relative inclinations $< 40°$. Note that systems with relative inclinations $> 140°$ are also dynamically stable. Although such retrograde orbits are unlikely on theoretical grounds, our conclusions are robust to this possibility; since the secular perturbation theory averages over the orbits it is also valid for retrograde orbits.

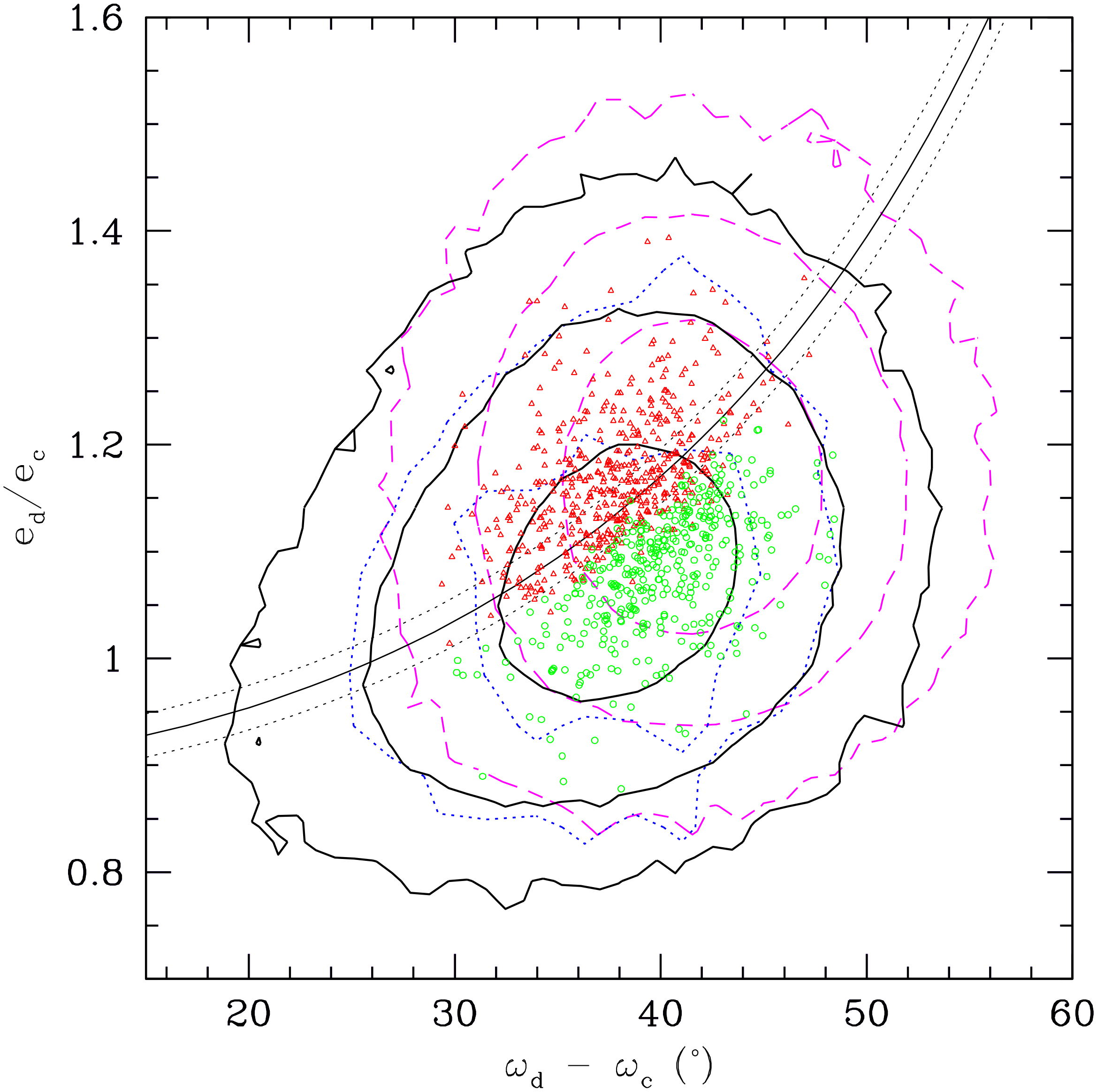

Fig. 5.— Observational constraints on the secular evolution parameters. The eccentricity ratio is plotted as a function of the difference between arguments of pericenter for planets c and d, all at present epoch. We show the 1-, 2-, and 3-σ contours for the posterior probability distribution function marginalized over the remaining fit parameters. The thick contours assume that the radial velocity variations are the result of three non-interacting Keplerian orbits viewed edge-on, while the dotted contours include the mutual gravitational interactions of the planets when fitting to the radial velocity data (only 1- and 2-σ contours are shown). The thin solid line shows the separatrix between librating (upper left) and circulating (lower right) solutions according to the classical second-order perturbation theory (neglecting the inner planet b). The dotted lines on either side show the variation in the location of the separatrix due to the uncertainty in the remaining orbital elements. The data points show the results of our direct numerical integrations for the full three-planet system: triangles (squares) indicate that the system was found to be librating (circulating). Noth that, regardless of the assumptions, the separatrix runs right through the 1-σ contours.

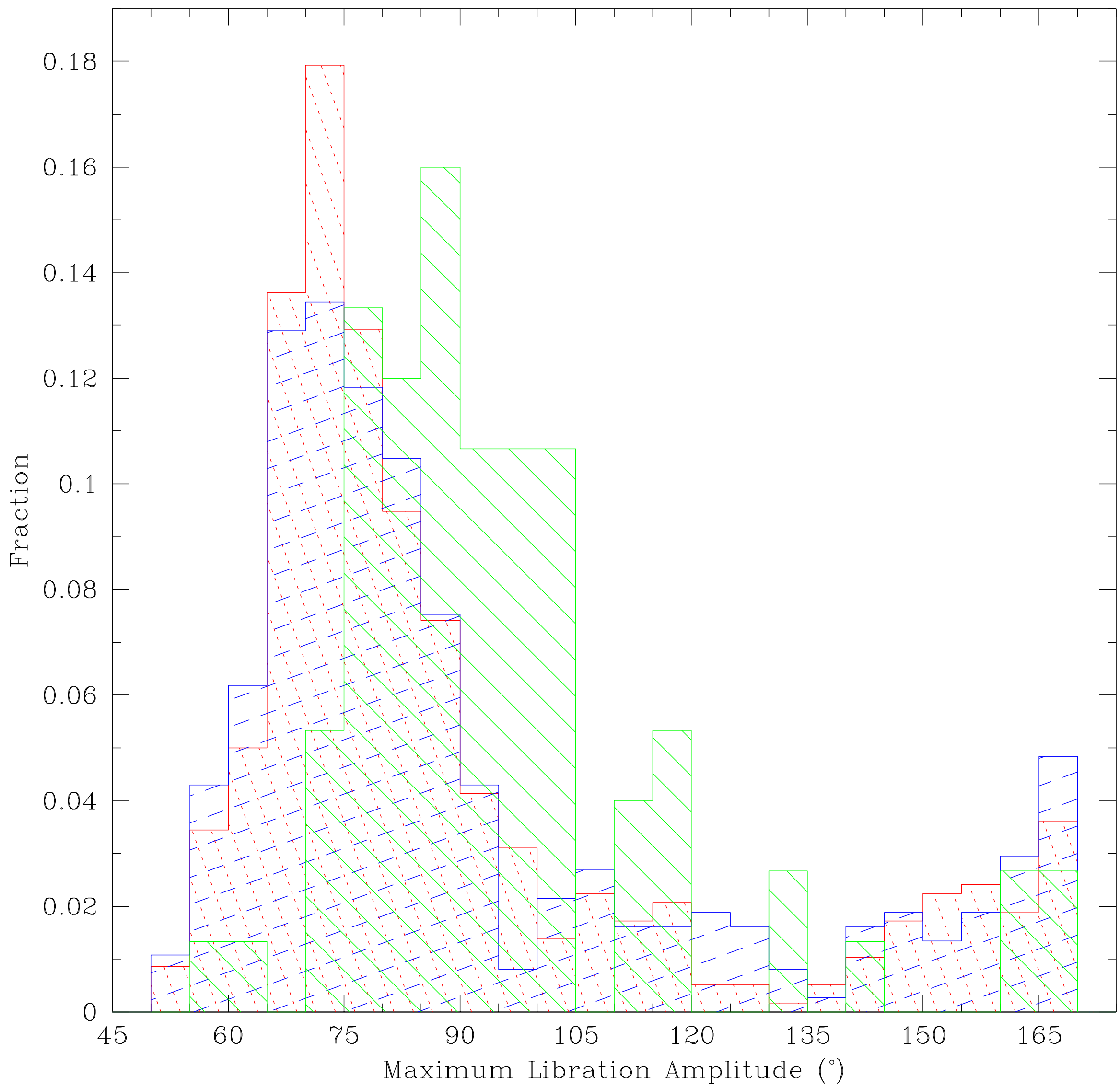

Fig. 6.— Histogram of maximum libration amplitudes for stable, librating systems of three sets of 1000 integrations. The histogram filled in with the solid line represents data from set #1, the dashed line is data for set #2, and the dotted line is data for set #6 in Table 3. Note that all systems are librating with relatively large amplitudes of libration, and that most are near 90°. The mean amplitude of libration for all stable librating systems was 80°.

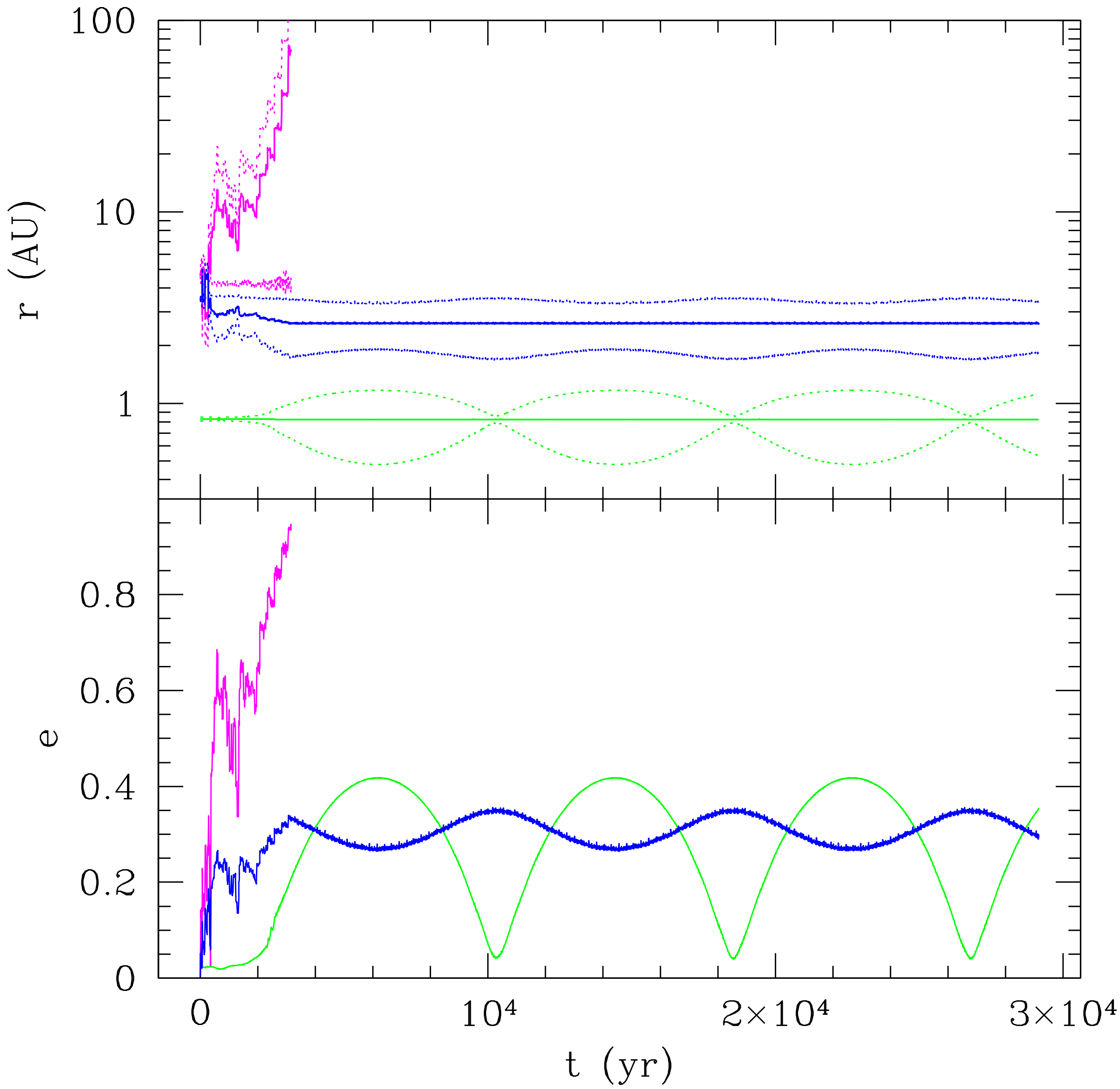

Fig. 7.— Dynamical evolution of a hypothetical planetary system similar to υ And with one additional planet. The top panel displays orbital eccentricities and the bottom panel shows semimajor axes for planets c, d, and e. In both panels the secular evolution for planet c is represented by the dashed line, planet c is the dotted line, and planet e is the solid line. After a brief period of dynamical instability, one planet is ejected, leaving the other two in a configuration very similar to that of υ And c and d. The innermost planet was not included, as it plays a negligible role.

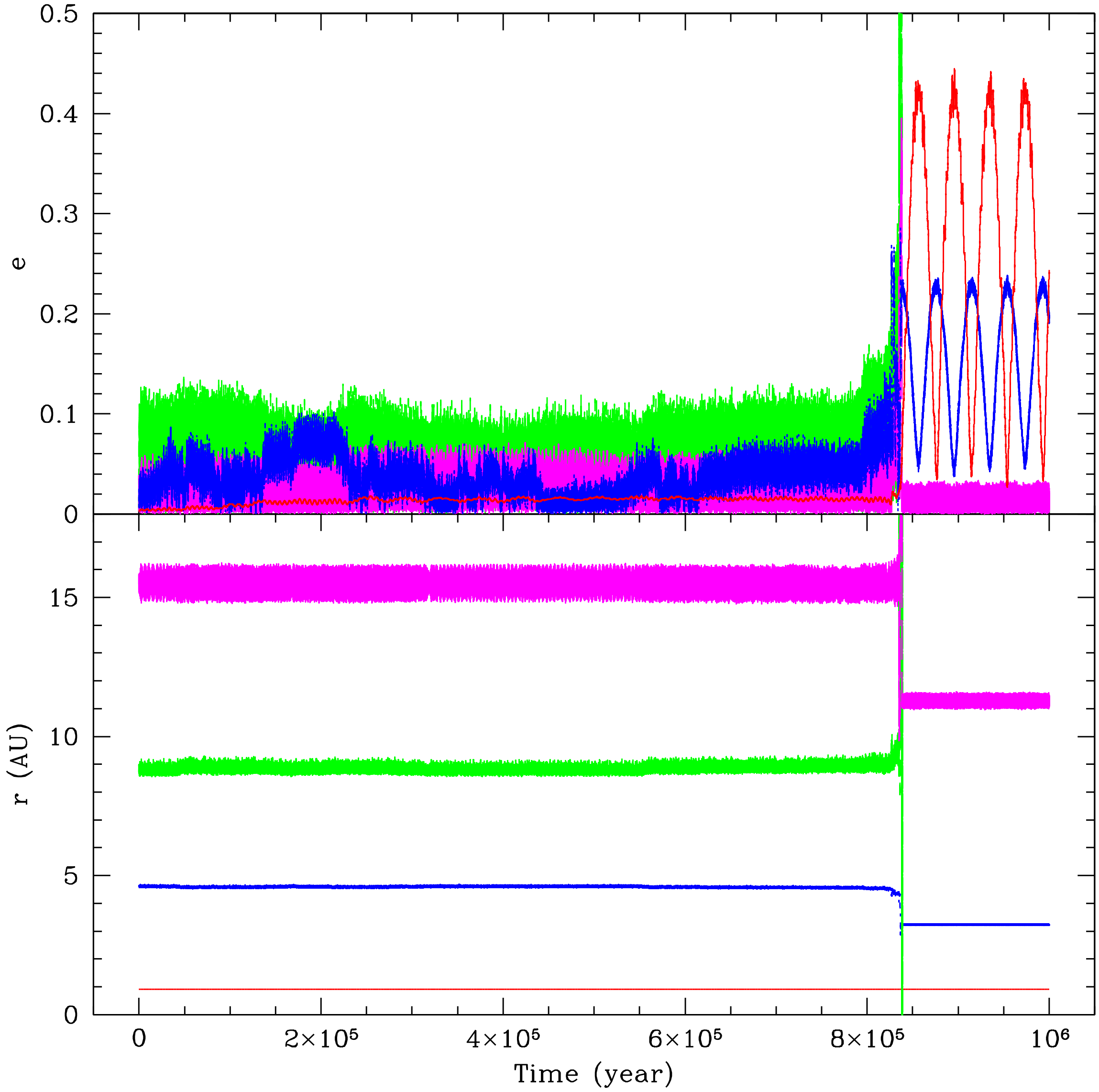

Fig. 8.— Evolution of a hypothetical planetary system similar to υ And with two additional planets. The top panel shows orbital eccentricities and the bottom panel indicates semimajor axes for planets c, d, e, and f, versus time. The system evolves in a seemingly quiet manner for more than 800, 000 years, when in a span of $\sim 15,000$ years planets e and f interact strongly with eachother and planet e is consequently ejected from the system. Planet f briefly perturbs d in the course of its strong interaction with planet e, imparting a finite eccentricity to it. Finally when e is ejected from the system, planet d is left with an eccentricity oscillating with small amplitude, though in a lower range than the present observed orbital eccentricity, and planet b's eccentricity is left with a large amplitude of oscillation, returning periodically to a nearly circular orbit. Note that planet f is left with a very small eccentricity after planet e is ejected.